Recent improvement in the KMS global marine gravity field

O. B. ANDERSEN[1], P. KNUDSEN[1], S. KENYON[2] and R. TRIMMER[2]

[1] *Kort- og Matrikelstyrelsen, Geodesy, Copenhagen, Denmark*
[2] *National Imagery and Mapping Agency, St Louis, USA*

Abstract. During the first half of 1998, the procedure for deriving the KMS global marine gravity field (Andersen and Knudsen, 1995, 1996) was revised. The resolution was enhanced, and several parameters were tuned to obtain a better gravity field. The updated procedure for the new KMS98 gravity field and their differences with the procedure for deriving the older KMS96 gravity field is presented in this paper. An important tool in the improvement of the KMS gravity field was the use of high quality marine gravity observations to check possible finetuning of parameters. Testing and comparison with other recent global marine gravity fields is carried out in regions of rapid changing gravity signal like over trenches and sea mounts to illustrate the improvement in the new gravity field. The improvements involved a better spatial varying filter for the interpolation of the geoid anomalies depending on the local RMS variability, and an enhanced filtering in the conversion between geoid anomalies and gravity. The KMS98 gravity field is available at the Internet-address: ftp://ftp.kms.dk/pub/GRAVITY, which also contains information on how to use the field.

1. Introduction

During the last decade the Earth's surface has been monitored from satellite altimetry from several satellites. These are Geosat (1985-1989), ERS-1 (1991-1996), TOPEX/POSEIDON (1992 ->) and ERS-2 (1995 ->). The radar altimeter measures the distance from the satellite to the sea surface and reveals changes in the ocean surface heights. If the oceans were motionless, the shape of its surface would be determined entirely by the gravitational attraction of the Earth. Even in that case, however, the sea surface would have hills and valleys.

A new version of the Andersen and Knudsen global marine gravity field, called the KMS98

Corresponding author: Ole B. Andersen; Kort og Matrikelstyrelsen, Geodesy, DK 2400 Copenhagen NV, Denmark; phone: +45 3587 5255; fax: +45 3587 5052; e-mail: oa@kms.dk

gravity field, is presented in this paper. This field is registered on a 2 by 2 minute grid. The grid interval was enhanced compared with older KMS gravity fields, which were registered on 3.75 by 3.75 minutes.

The gravity field covers all marine regions between the 82° S and 82° N parallels, where ERS-1 satellite altimetry data were available. In the region limited by the 72° S and 72° N parallels, Geosat satellite data were also included. The spacing between the ERS-1 ground tracks at the Equator is almost constantly 8 km. The Geosat ground tracks are generally 1.5 times denser than ERS-1, however, they are much more unevenly spaced than ERS-1.

2. Data editing and processing

In this section, the derivation of the KMS98 gravity field will be described with special emphasis on the improvements over the older KMS96 gravity field. (Andersen and Knudsen, 1996, 1997).

The altimeter data from both geodetic missions are obtained as the usual 1-s mean values with an along-track spacing of about 7 km. To enhance the quality of the altimetry, both data sources applied the newest set of orbits similar for the two geodetic missions. Here Geosat applied the new recomputed orbits based on the JGM-3 gravity model, (Tapley et al., 1996) and ERS-1 applied the JGM-3 orbits provided by the Delft Institute of Technology. The correction for atmospheric, tropospheric path delay and geophysical corrections closely follows that of KMS96. Data were removed if any of the applied range corrections were absent except the ocean tide correction. Similarly data were removed if the standard deviation of the height observations exceeded 0.3 m. This resulted in about 30 million altimeter data from the Geosat and about 20 million altimeter data from the ERS-1 geodetic missions.

From this point on all subsequent processing and derivation of the gravity field was carried out in small cells of the size of 2° latitude by 10° longitude. Globally, this mosaic has 80 times 36 cells (latitude by longitude) equivalent to 2880 cells (Fig. 1 illustrates the global mosaic of the cells). Observations were extracted in a somewhat larger cell by extending the cell with a border zone of 0.5° latitude by 1° longitude. This extended cell is then of size 3° latitude by 12° longitude. The selection of such small subareas was essential to the modelling of orbit errors and sea surface variability. A choice of larger cells caused problems in the removal of these signals, while smaller cells may corrupt parts of the regional geoid signal.

To reduce the effects of residual orbit errors and sea surface variability, the tracks were initially fitted individually to the joint NASA Goddard Space Flight Center and NIMA geoid model EGM96 (Lemoine et al., 1997) by estimating bias and tilt terms to each track, thus removing all signals with a wavelength longer than about 3°-4°. Subsequently, a crossover adjustment of the tracks was carried out, also using bias and tilt terms (e.g., Knudsen and Brovelli, 1993). To avoid problems with rank deficiency, a minimum variance criterion was applied.

Hereafter, each height observation was compared with an estimated height to detect outliers and gross errors. As in work by Tscherning (1990), the estimate was obtained using least squares collocation. That is,

$$\hat{h}_P = \mathbf{c}_P^T (\mathbf{C} + \mathbf{D})^{-1} \underline{h}, \tag{1}$$

where C and D are signal and error covariance matrices, c_P is a vector of the covariances between the estimate and the observations, and $\underline{h}$ contains the 20 nearest observations (5 in each quadrant around the estimation location). The observation itself entered the estimation with its standard deviation increased to 1 m. As a covariance function, a second-order Markov covariance function is used like

$$c(r) = C_0 \left(1 + \frac{r}{\alpha} \right) e^{(-r/\alpha)}, \tag{2}$$

where r is the lag and C_0 is the signal variance. The parameter α was fixed so that the correlation length (where a 50% correlation is obtained) was 30 km to ensure a relatively smooth interpolation. Then a screening for gross errors, e.g., observations affected by sea ice, was carried out. This was done by removing observations with a discrepancy between the observed and the estimated height exceeding 1 m (Andersen et al., 1996).

This screening reduced the number of data by roughly one percent. Finally, the whole process is repeated using this reduced data set. This includes the fitting to the geoid model EGM96 and the crossover minimization, as this process might be contaminated by outliers and gross errors that might have affected the initial adjustment. Consequently, most of the permanent parts of the sea surface topography have been reduced. Until this stage, the data-processing has been identical to the processing used for the KMS96 gravity field.

3. Mapping of the gravity field

The edited and adjusted altimeter data within each extended cell used for processing (3° latitude by 12° longitude) were interpolated onto a regular grid using an enhanced collocation method. As the fast Fourier transform (FFT) was chosen for the conversion between geoid and gravity anomalies, it was required that the data be distributed in a regular grid. The FFT method is a very efficient approximation method, but it is not a very rigorous method. However, computational constraints makes this one of the only feasible methods because of the size of the data set and the required resolution.

This conversion from geoid into gravity anomalies enhances high frequencies, and consequently results may be sensitive to cross-track gradients caused by sea surface variability arising as the distance between parallel tracks becomes very small in the geodetic mission altimetry. Such effects may be reduced by using altimetric slopes or second-order derivatives (e.g., Sandwell and Smith, 1997; Hwang and Parsons, 1995). Another way of limiting the influence of the surface variability, which may cause erroneous cross-track gradients between parallel tracks, is to model this error by adding an additional covariance function for this error in

X-over RMS from geodetic mission altimetry

5.0 ▮▯ 20.0 cm
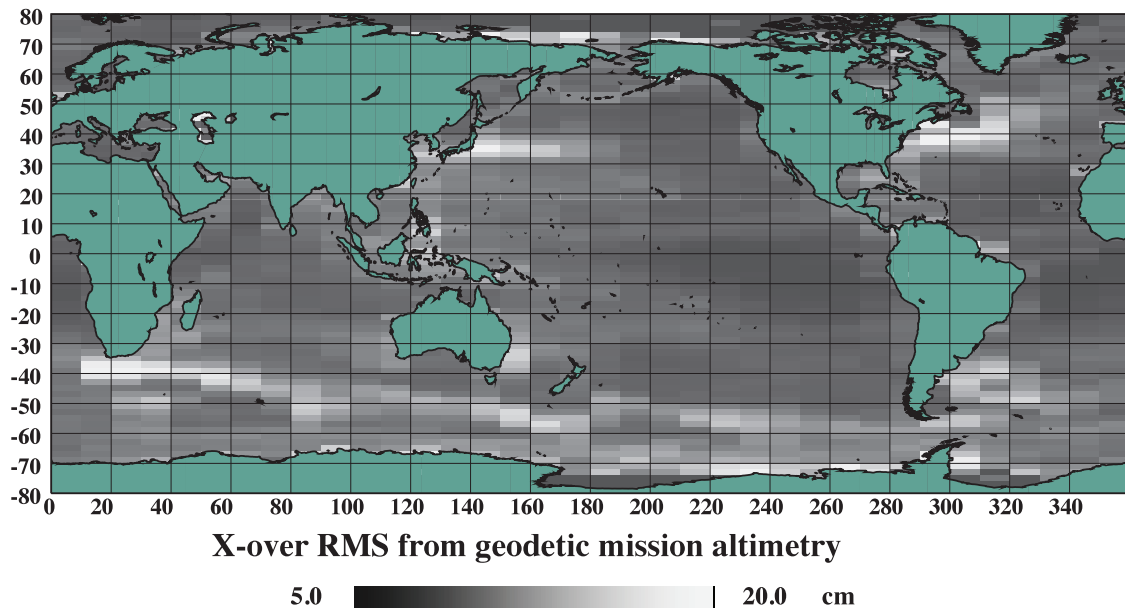
Fig. 1 - Global distribution of RMS crossover discrepancies cell by cell in the KMS gravity field.

the interpolation procedure. This error covariance function was applied to observations on the same track only, assuming the error to be temporally uncorrelated. Hence, for observations on the same track, a covariance function like

$$c(r) = C_0 \left(1 + \frac{r}{\alpha}\right) e^{(-r/\alpha)} + D_0 \left(1 + \frac{r}{\beta}\right) e^{(-r/\beta)}, \tag{3}$$

was used. The parameters for this interpolation were changed between the KMS96 gravity field and the new KMS98 gravity field.

For the KMS96 gravity field the parameters D_0 and β were empirically determined globally, to a variance of $(0.1 \text{ m})^2$ and a correlation length of 100 km, respectively. For observations on the same track, D_0 was fixed at zero yielding an expression similar to (2). C_0 was always fixed at $(0.2 \text{ m})^2$, and the parameter α was fixed so that the correlation length was 15 km.

For the KMS98 gravity field this process was enhanced. Instead of using a fixed global value for D_0 the value was estimated locally depending on the local conditions. This was carried out using the crossover discrepancies between all tracks in the processing cell.

In Fig. 1 the distribution of crossover RMS values estimated for each of the 2° E latitude by 10° E longitude processing cell is shown. The RMS of the crossover discrepancies varies between 0.05 meters and 0.20 meters, being largest in the major eastern boundary currents. Consequently the variance D_0 varies between $(0.05 \text{ m})^2$ and $(0.20 \text{ m})^2$. The correlation length was maintained at a fixed value of 100 km. As usual, D_0 was fixed at zero for observations on the same track. Similarly, C_0 was kept fixed at $(0.2 \text{ m})^2$. However, the correlation length

parameter α was increased to 17 km in order to smooth the gravity field a bit more than for the KMS96 gravity field.

In the collocation estimation (Eq. 3) the 48 nearest observations are used to secure redundant geoid information at crossing tracks. The result of the gridding is a 1/30° by 1/30° grid extended by a border zone of 1° latitude by 3° longitude around the processing cell, to avoid spectral leakage in the following steps. This resulting grid of geoid undulations were then converted into gravity anomalies, Δg, using Fast Fourier Transform (FFT) (Schwarz et al., 1990). In the frequency domain (u,v), the geoid anomalies $\tilde{N}(u,v)$ is related to the gravity anomalies $\Delta g(u,v)$ like

$$\Delta \tilde{g}(u,v) \approx \omega \ \gamma \ \tilde{N}(u,v) \ F(\omega), \tag{4}$$

where $\omega^2 = u^2 + v^2$ and γ is the normal gravity. Such a transformation from geoid undulations into free-air gravity anomalies is a differentiation that enhances the high frequencies. As a consequence, it is sensitive to noise. Therefore, a Wiener filtering function, $F(T)$, was introduced in (4). This filter function is equivalent to a collocation filter that assumes Kaula's rule to be valid and that assumes uncorrelated noise (details by Forsberg and Solheim, 1988). That is,

$$F(\omega) = \frac{\omega_c^4}{\omega^4 + \omega_c^4}, \tag{5}$$

for the KMS96 gravity field the "cutoff" frequency, T_c, where the filter is 0.5, was empirically determined to a wavelength of 12 km, which roughly corresponds to about 10 cycles per degree or harmonic degree 3600.

For the KMS98 gravity field, comparisons with high quality marine gravity carried out by the National Imagery and Mapping Agency (NIMA) opened for possible fine-tuning of this "cutoff" frequency. Initially, it was found that 11 km gave the best result. But by increasing the correlation length from 15 to 17 km in the interpolation of the geoid anomalies prior to the conversion to gravity, this "cutoff" frequency could be lowered to 10.5 km.

Before the Fourier transform of the geoid grid was computed, a cosine taper was applied in the outer 0.5° parts of the grid. This was done to avoid spectral leakage caused by wavelengths that are not periodic within the area. Subsequently, the contribution of the EGM96 gravity field was restored to obtain the free air gravity anomalies, and the gravity field was isolated within the small 2° by 10° cell. Finally, all cells were merged together to obtain the final global marine gravity field.

4. Comparison with marine gravity

Comparisons with marine free air observations were made in three different regions of the world. The first two regions are regions of very large gravity gradients. The last region is a region with a very large gravity signal.
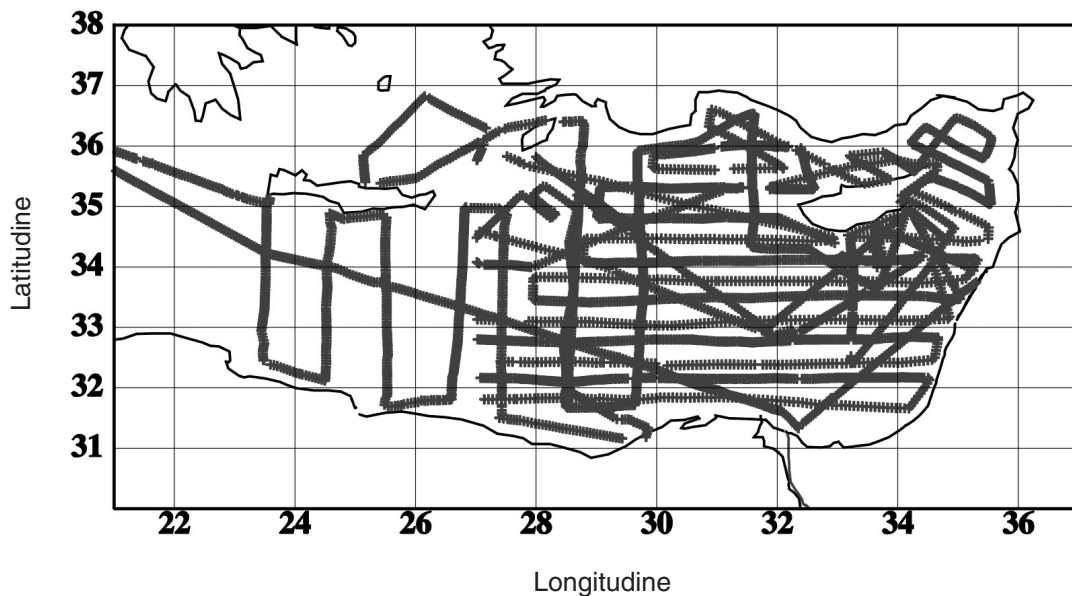
Fig. 2 - Location of 4151 marine gravity observations in the eastern Mediterranean from Morelli et. al. (1975).

The first two regions of large gravity gradients were chosen as they have very difficult gravity to model, and should be regions, where the KMS gravity field is supposed to have problems. This is because the KMS gravity field is sensitive to cross-track gradients as the distance between parallel tracks becomes small. This is again caused by the fact that height measurements and not along-track slopes are used in the derivation of the gravity field.

Both comparisons also showed that the Sandwell and Smith gravity field performed better than the old KMS96 gravity field in these test regions. This is partly explained by the fact that the Sandwell and Smith gravity field is not smoothed as much as the old KMS gravity field. However, the fine-tuning of the parameters in the derivation of the KMS98 gravity field, dramatically enhanced the modelling of the high frequencies in the gravity field signal. Consequently, the result now compares better than the Sandwell and Smith gravity field in regions of a rapid changing gravity signal. Other comparisons in favour of the KMS98 gravity field in other regions of the world have been presented by Andersen (1997, 1998) and

Table 1 - Comparison with NIMA gravity observations in a 3° by 3° area over steep ridge. Totally 14 665 comparisons. All values are in mGal.

	KMS96 (3.75')	**Sandwell 7.2 (2')**	**KMS98 (2')**
Mean	-0.63	1.16	-0.66
Std dev	6.89	5.65	5.31
Min	-68.61	-54.98	-53.81
Max	24.28	20.16	19.18
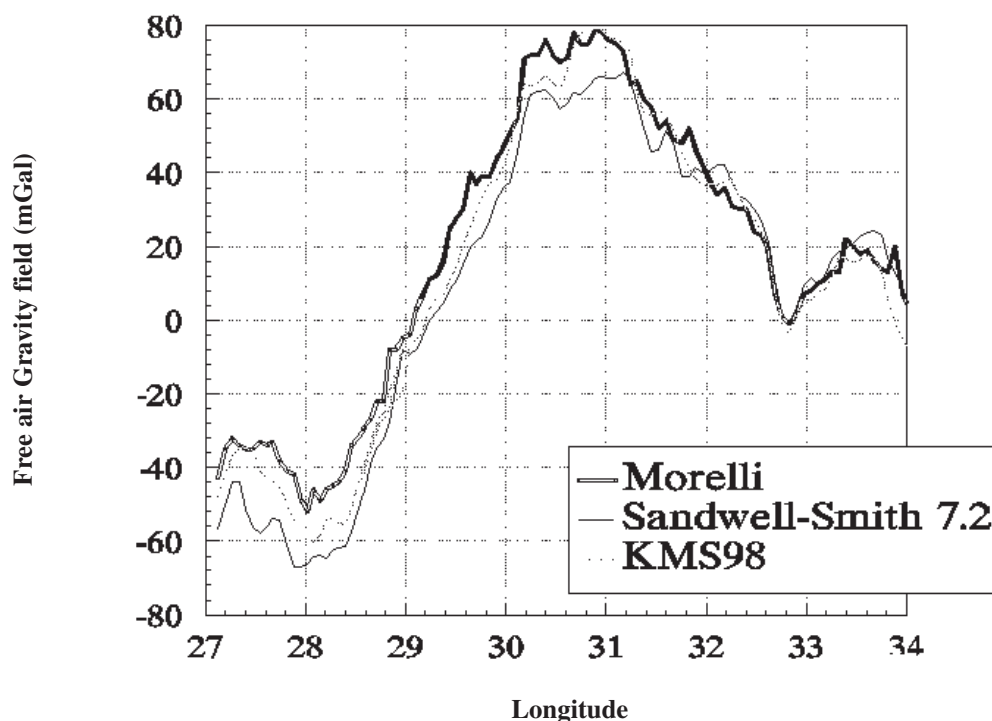
Fig. 3 - Direct comparison between the Morelli marine gravity observations, the Sandwell and Smith (v 7.2) and the KMS98 gravity field are plotted along the southern east-west survey-line in Fig. 2.

Behrend et al. (1997).

In the comparisons in Table 1 the Sandwell and Smith version 7.2 of the global marine gravity field has been used (Sandwell and Smith, 1997). The marine gravity anomalies have been gridded on a Mercator projection giving it a variable latitude spacing and a constant longitude spacing of 1/30°. Therefore, the provided software program "interp_ship" was used to interpolate towards the positions of marine gravity observations. Version 7.2 used in this study was derived from the following data sources: All ERS-1 GM data (two 168-day cycles Ocean Product) all GEOSAT/GM data, stack of 62 repeat cycles of GEOSAT/ERM, and a stacks of 16 repeat cycles of ERS-1 35-day repeats.

Table 2 - Comparison in a 2° latitude by 5° longitude area over cluster of sea mounts. 15 748 comparisons totally. All values are in mGal.

	KMS96 (3.75')	Sandwell 7.2 (2')	KMS98 (2')
Mean	-1.59	-0.89	-1.39
Std dev	6.80	5.87	5.46
Min	-41.35	-37.46	-31.94
Max	26.82	32.18	26.69

Table 3 - Comparison with 4151 gravity observations in the eastern Mediterranean Sea. The positions can be found in Fig. 2.

	KMS96 (3.75')	Sandwell 7.2 (2')	KMS98 (2')
Mean	-1.12	-6.61	-1.03
Std dev	9.71	18.96	8.97
Min	-66.15	123.25	-61.44
Max	42.11	57.92	36.93

Finally, a comparison in a region of very large gravity anomalies was carried out. This comparison with marine gravity data was done with a set of 4151 gravity observations in the eastern Mediterranean Sea by Morelli et al. (1975). The location of the stations is shown in Fig. 2 and the comparison is tabulated in Table 3. This region has a very large gravity signal and the marine observations range from -218 mGal to 116 mGal.

In Fig. 3 the gravity field along the southern east-west gravity profile between (31.8° N 34.2° E and 31.8° N, 27.1° E) from the Morelli observations, the Sandwell and Smith gravity field and the KMS98 gravity field are shown. Both the KMS98 and the Sandwell and Smith gravity field has a trend compared with the Morelli data with small discrepancies in the eastern part, but large differences in the western part. Here, the Sandwell and Smith gravity values are around 20-25 mGal lower that Morelli data whereas the KMS values are 5-10 mGal lower.

The standard deviations with this data set is around 9-10 mGal with the Sandwell and Smith data set having a very large standard deviation of 18.9 mGal. Similarly, the Sandwell and Smith gravity field have a systematic mean difference of 6.6 mGal. The cause of this has not been investigated, but the estimation of the medium to long wavelength parts of the gravity field may suffer when using slopes in enclosed seas as done by Sandwell and Smith.

5. Summary - Future work

The improved KMS98 global marine gravity field has been presented here. The field is presented on a finer resolution grid, and several parameters were tuned to obtain a better gravity field with respect to mapping of small scale features in the gravity field. The improvements involved a better spatial varying filter for the interpolation of the geoid anomalies depending on the local RMS variability, and an enhanced filtering in the conversion between geoid anomalies and gravity.

Several improvements are foreseen in the near future leading to a new global gravity field (KMS99). The distance between parallel tracks is now down to 4-6 km, whereas the distance between measurements along track is roughly 7 km using the 1-sec mean anomalies. The along-track resolution can be enhanced by a factor of two by using 1/2-sec mean anomalies. Similarly, data from the ERS-1 and ERS-2 Exact Repeat Missions (ERM) have not been considered so far, but it is expected that these data sets could lead to improvement in the spatial coverage at high latitudes.

Several investigations (H.-G. Wenzel, personal communication) have shown that the de-

spiking procedure should be tuned better, as some anomalous large gravity values can be found very close to the coast. Similarly the use of a constant "cutoff" frequency in the Wiener Filtering should be considered. Studies have already been carried out and it is expected that a new version (KMS99) will be released during the summer of 1999.

References

Andersen O. B. and Knudsen P.; 1998: *Global Marine Gravity Field from the ERS-1 and GEOSAT Geodetic Mission Altimetry*. J. Geophys. Res., **103**, 8129-8137.

Andersen O. B., Knudsen P. and Tscherning C. C.; 1996: *Investigation of methods for global gravity field recovery from dense ERS-1 geodetic mission altimetry*. In: Rapp, Cazenave and Nerem (eds), Global Gravity Field and its temporal variations. IAG Symposia no. 116, Springer Verlag, Berlin Heidelberg, p. 218-226.

Andersen O. B. and Knudsen P.; 1995: *Global gravity field from the ERS-1 geodetic mission*. Earth Observation Quarterly, **47**, ESRIN, 1-5.

Behrend D., Denker H. and Schmidt K.; 1996: *Digital gravity data sets for the Mediterranean Sea derived from available maps*. Bull. d'Information, 78, BGI, Touluse Cedex, France, 32 – 41.

Forsberg R. and Solheim D.; 1988: *Performance of FFT methods in local gravity field modelling*. In: R. H. Rapp (ed), Proc. Chapman conference on progress in the determination of the Earths gravity field, Ft. Lauderdale, Florida, USA, 100-103.

Hwang C. and Parsons B.; 1995: *Gravity anomalies derived from Seasat, Geosat, ERS-1, and TOPEX/POSEIDON altimetry and ship gravity: A case study over the Reykjanes Ridge*. Geophys. J. Int., **122**, 551-568.

Knudsen P. and Brovelli M.; 1993: *Collinear and Cross-over Adjustment of Geosat ERM and Seasat altimeter data in the Mediterranean Sea*. Surveys in Geophysics, **14**, 449-459.

Lemoine F. G., Smith D. E., Kunz L., Smith R., Pavlis E. C., Pavlis N. K., Klosko S. M., Chinn D. S., Torrence M. H., Williamson R. G., Cox C. M., Rachlin K. E., Wang Y. M., Kenyon S. C., Salman R., Trimmer R., Rapp R. H. and Nerem R. S.; 1997: *The development of the NASA GSFC and DMA joint geopotential model*. In: Proc. Int. Symposium on Gravity geoid and Marine Geodesy, Japan, Sept, **117**, 461-469.

Morelli C., Pisani M. and Gantar C.; 1975: *Geophysical studies in the Aegean sea and in the Eastern Mediterranean*. Boll. Geofis. Teor. App., **XVIII**, 127-168.

Sandwell D. T. and Smith W. H. F.; 1997: *Marine gravity anomaly from Geosat and ERS-1 satellite altimetry*. J. Geophys Res., **192**, 10 039-10 054.

Tapley B. et al.; 1996: *The Joint Gravity Model 3*. J. Geophys. Res., **101**, 28 029-28 049.

Tscherning C. C.; 1990: *A strategy for gross-error detection in satellite altimeter data applied in the Baltic Area for enhanced geoid and gravity determination*. In: R. H. Rapp and F. Sansó (eds), Determination of the Geoid - Present and Future, IAG Symposia 106, Springer Verlag, Berlin Heidelberg.